Chinese Chemical Letters 35 (2024) 108832

Contents lists available at ScienceDirect

Chinese Chemical Letters

journal homepage: www.elsevier.com/locate/cclet

Unveiling inverse vulcanized polymers as metal-free, visible-light-driven photocatalysts for cross-coupling reactions

Lang Gao[a], Cen Zhou[b,*], Rui Wang[a], Feng Lan[a], Bohang An[a], Xiaozhou Huang[a], Xiao Zhang[a,*]

[a] *Fujian Key Laboratory of Polymer Science, Fujian Provincial Key Laboratory of Advanced Materials Oriented Chemical Engineering, College of Chemistry and Materials Science, Fujian Normal University, Fuzhou 350007, China*

[b] *Fujian Engineering and Research Center of New Chinese Lacquer Materials, College of Materials and Chemical Engineering, Minjiang University, Fuzhou 350108, China*

ARTICLE INFO

Article history:
Received 1 May 2023
Revised 10 July 2023
Accepted 24 July 2023
Available online 25 July 2023

Keywords:
Cross coupling
Inverse vulcanized polymers
Metal free
Photocatalyst
Visible light

ABSTRACT

Inverse vulcanized polymers (IVPs) that generated from elemental sulfur and smaller amounts of alkenes have found broad promising applications such as cathode materials for Li-S batteries, dynamic and repairable materials, optics applications, and metal sorption. However, their exploration in organic synthesis is still unprecedented. Here we first report the application of inverse vulcanized polymers in catalysis for organic transformations. A biomass-derived inverse vulcanized polymer (IVP-EAE) is found to be capable of catalyzing cross-coupling reactions in a transition-metal-free fashion under visible light. This method allows the direct C–H functionalization of pyrroles and *N*-arylacrylamides with (hetero)aryl halides, respectively, leading to the formation of two sets of structurally important scaffolds including pyrrole-containing biaryls and 3,3′-disubstituted oxindoles with high selectivity. We anticipate this study will not only unveil the new potential of IVPs, but also offer a distinct type of catalysts for organic transformations.

In modern society, synthetic polymers play crucial roles in our daily life [1]. However, the vast majority of synthetic polymers are derived from non-renewable petrochemicals, which imposes a significant threat on the sustainability of environment [2,3]. It is therefore urgent to investigate high-performance polymers that are generated from renewable biomass or industrial waste [4,5]. As an unwanted by-product of petroleum refining and gas reserves, elemental sulfur (S_8) is produced in about 70 million tons annually with very little consumption [6]. Megaton quantities of S_8 have been stockpiled on the ground for decades and continuingly accumulated each year. In this regard, the emergence of organic polymers synthesized from S_8 and alkenes *via* inverse vulcanization has gained extensive interest (Scheme 1, top) [7–13]. Since the pioneering work of Pyun and co-workers in 2013 [14], inverse vulcanized polymers (IVPs) have found wide applications such as cathode materials for Li-S batteries [14–16], dynamic and repairable materials [17], optics applications [18], and metal sorption [19,20]. A wide range of structurally and electronically diverse unsaturated compounds have been used as the organic comonomers, which include those derived from conventional petrochemicals, renewable resources, and abundant industrial by-products. Despite the notable advances, the utilization of IVPs in organic synthesis remains previously elusive.

Structurally, inverse vulcanized polymers (IVPs) have high percentage of S-S bonds. The ability of each sulfur atom to accept two electrons makes IVPs exhibit excellent redox reactivity. Meanwhile, the diverse co-polymerized alkenes offer flexible handles for tuning properties [7–13]. Inspired by these intriguing redox properties of IVPs for Li-S batteries, we were curious about the behavior of IVPs upon visible-light irradiation and wondered whether IVPs could be unveiled as a new class of photocatalysts to convert abundant solar energy into chemical energy [21–36].

Here we investigate the photophysical properties of IVPs and disclose the first implementation of IVPs for synthetic chemistry (Scheme 1, bottom). Under visible-light irradiation, an eugenol allyl ether-derived inverse vulcanized polymer (IVP-EAE) is found to be capable of catalyzing cross-coupling reactions of readily available (hetero)aryl halides with pyrroles and *N*-arylacrylamides, respectively. Two sets of structurally important scaffolds including pyrrole-containing biaryls and 3,3′-disubstituted oxindoles are fur-

---

* Corresponding authors.
E-mail addresses: zhoucen@mju.edu.cn (C. Zhou), zhangxiao@fjnu.edu.cn (X. Zhang).

https://doi.org/10.1016/j.cclet.2023.108832

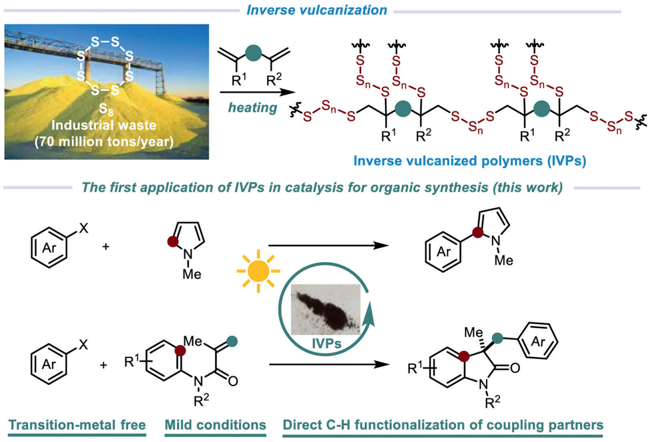

Scheme 1. The first application of inverse vulcanized polymers in catalysis for organic synthesis.

nished in a transition-metal-free fashion. We report our results from this study.

At the beginning, several representative IVPs including the firstly disclosed IVP-DIB [14,15], industrial by-product-derived IVP-DCPD [37], and renewable resource-derived [38] IVP-EG as well as IVP-EAE, which can be accessed *via* inverse vulcanization (IV) reactions between elemental sulfur and the corresponding alkenes namely 1,3-diisopropenylbenzene (DIB), dicyclopentadiene (DCPD), eugenol (EG) [39], and eugenol allyl ether (EAE) [39] were chosen (Scheme 2a).

To gain insights into the optical properties of these inverse vulcanized polymers, standard characterizations were performed (Schemes 2b-e). As illustrated in Scheme 2b, the solid-state UV–vis diffuse reflectance spectra (DRS) showed that all the above IVPs display visible-light absorption, although vary dramatically. Gratifyingly, the transient photocurrent experiments indicated that IVPs uniformly possess rapid photocurrent response upon visible light irradiation (Scheme 2c). Among which, IVP-EAE is more apparent than the other three. Consistently, the Nyquist curve of IVP-EAE exhibited a relatively smaller radius in the electrochemical impedance spectroscopy (EIS), suggesting a lower interfacial charge transfer resistance in IVP-EAE (Scheme 2d). Collectively, these two experiments pointed out the feasibility of photogenerated charge separation and transfer in IVPs. Moreover, the time-resolved PL decay spectroscopy showed that the average PL lifetimes of IVP-DIB, IVP-DCPD, IVP-EG, and IVP-EAE is 2.18, 2.54, 2.58, and 3.13 ns, respectively (Scheme 2e).

Encouraged by the above-mentioned photophysical properties of IVPs, we next explored their potential application in visible-light photocatalysis. Cross-coupling reactions are broadly used in both academia and industry for the synthesis of high-value molecules that range from biologically active targets to organic materials [40–42]. Although powerful, traditional cross-couplings typically require the use of palladium complexes as catalysts, two prefunctionalized partners, and elevated temperature [43]. Comparatively, photoredox catalysis offers a more sustainable and environmentally friendly approach [44] because it allows the direct cross-couplings of aryl halides with unprefunctionalized partners operated under mild reaction conditions [45–50]. Mechanistically, photoredox-catalyzed single-electron reduction of aryl halides affords aryl radicals, which add to another (hetero)arenes to generate biaryls followed by aromatization. As such, cross-coupling of aryl halides with *N*-methyl pyrrole was selected as the model reaction.

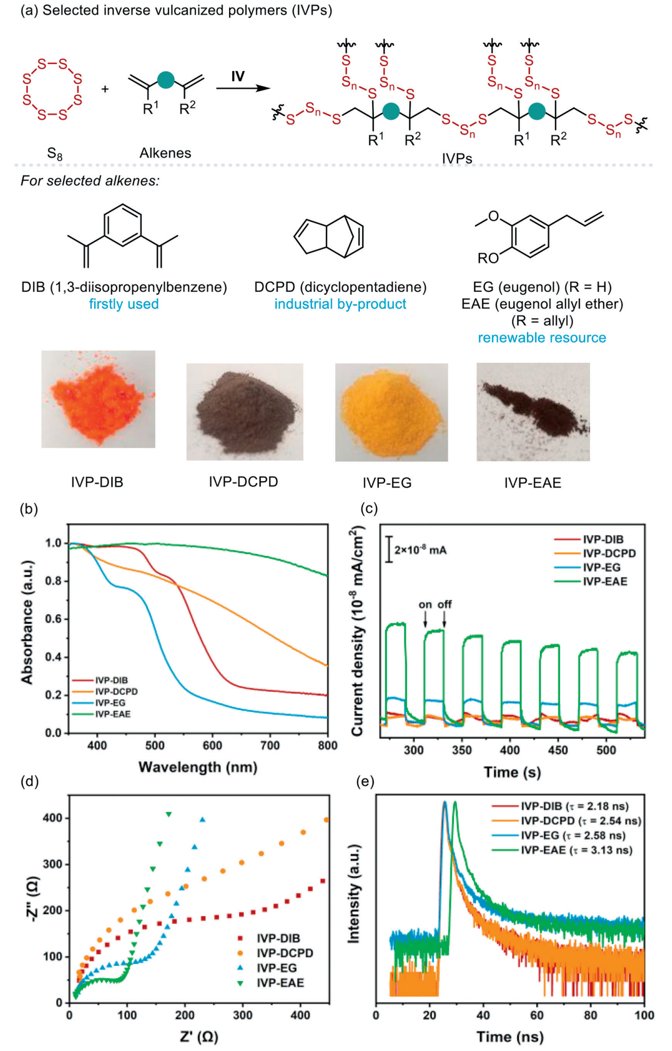

Scheme 2. (a) Inverse vulcanized polymers (IVPs) used in this study. (b) Solid-state UV–vis diffuse reflectance spectra (DRS) of selected IVPs. (c) Photocurrent tests of selected IVPs. (d) EIS Nyquist plots of selected IVPs. (e) Time-resolved PL spectra of selected IVPs.

We initiated our studies by testing the cross-coupling between 1-(4-bromophenyl)ethan-1-one (**1a**) and *N*-methyl pyrrole (**2**) under blue LEDs irradiation. Encouragingly, the desired reaction took place in the presence of all the selected IVPs and elemental sulfur using DMSO as the solvent, K_2CO_3 as the base, and H_2O as the additive (Table 1, entries 1–5). Among which, IVP-EAE gave the optimal yield (81%), which is consistent with its superior photophysical properties as shown in Scheme 2 (Table 1, entry 1). The solvents exerted important impact on the reaction outcomes. While CH_3CN and acetone proved viable, the use of MeOH, DCM, THF, or H_2O instead of DMSO as the solvent failed to give any conversion (Table 1, entries 6–8). Changing the base to Cs_2CO_3, Et_3N, or DBU led to inferior results (Table 1, entries 9–11). Decreasing the loading of *N*-methyl pyrrole (**2**) to 2 equiv. amounts resulted in a drop in the yield (Table 1, entry 12). Notably, the reaction did not proceed in the absence of a base, further demonstrating the crucial role of K_2CO_3 (Table 1, entry 13). Removing H_2O from the system resulted in a slightly decreased yield for this heterobiaryl coupling (72%, entry 14, Table 1). Finally, control experiments confirmed that IVP-EAE, inert atmosphere, and visible light are all crucial for the process, as their absence shut down the reaction severely (Table 1, entries 15–17).

With the optimized conditions in hand, the scope of (hetero)biaryl cross-coupling was evaluated. As shown in Scheme 3, a range of aryl halides bearing substituents at *para*-, *meta*-, and

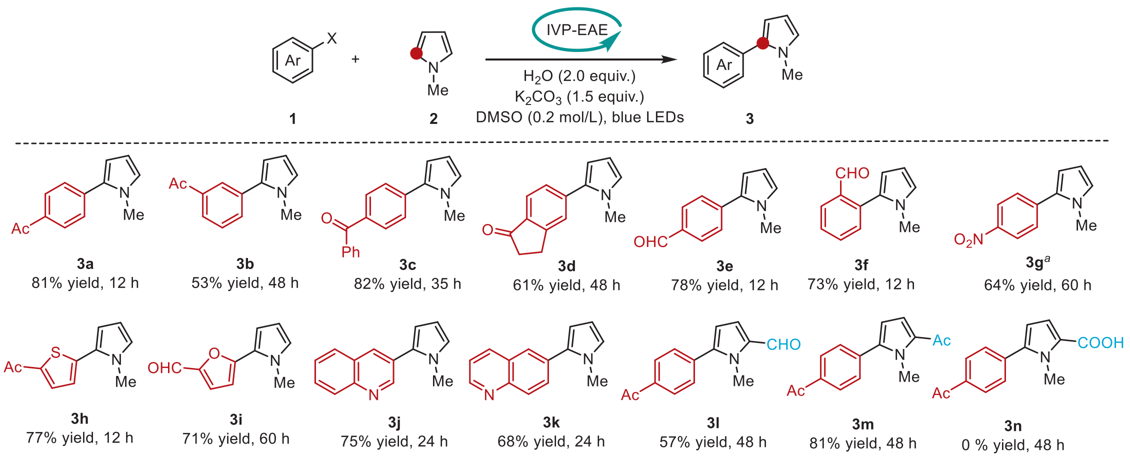

Scheme 3. Substrate scope for (hetero)biaryl cross-coupling. Reaction conditions: a solution of IVP-EAE (10.0 mg), **1** (0.2 mmol, 1.0 equiv.), **2** (4.0 mmol, 20.0 equiv.), H_2O (0.4 mmol, 2.0 equiv.), and K_2CO_3 (0.3 mmol, 1.5 equiv.) in DMSO (1.0 mL, 0.2 mol/L) was irradiated by blue LEDs (30 W) at room temperature under nitrogen atmosphere. Unless otherwise noted, (hetero)aryl bromides were used. Isolated yield. [a] 1-iodo-4-nitrobenzene was used.

Table 1
Optimization of the reaction conditions for (hetero)biaryl cross-coupling.[a]

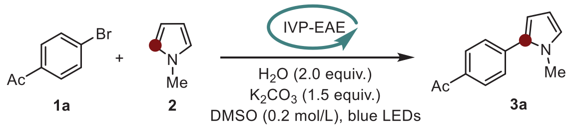

Entry	Variations from standard conditions	Yield (%)[b]
1	None	82 (81)[c]
2	IVP-DIB instead of IVP-EAE	24
3	IVP-DCPD instead of IVP-EAE	51
4	IVP-EG instead of IVP-EAE	10
5	S_8 instead of IVP-EAE	21
6	CH_3CN instead of DMSO	73
7	Acetone instead of DMSO	59
8	MeOH, DCM, THF, or H_2O instead of DMSO	0
9	Cs_2CO_3 instead of K_2CO_3	69
10	Et_3N instead of K_2CO_3	29
11	DBU instead of K_2CO_3	67
12	**2** (2.0 equiv.) was used	23
13	No K_2CO_3	0
14	No H_2O	72
15	No IVP-EAE	0
16	Air instead of N_2	4
17	No light	0

[a] Reaction conditions: a solution of IVP-EAE (10.0 mg), **1a** (0.2 mmol, 1.0 equiv.), **2** (4.0 mmol, 20.0 equiv.), H_2O (0.4 mmol, 2.0 equiv.), and K_2CO_3 (0.3 mmol, 1.5 equiv.) in DMSO (1.0 mL, 0.2 mol/L) was irradiated by blue LEDs (30 W) at room temperature under nitrogen atmosphere for 12 h.

[b] Determined by ^1H NMR yield using CH_2Br_2 as an internal standard.

[c] Isolated yield. DMSO = dimethylsulfoxide; DCM = dichloromethane; THF = tetrahydrofuran; DBU = 1,8-diazabicyclo[5.4.0]undec–7-ene.

ortho- positions were engaged in the arylation with *N*-methyl pyrrole (**2**) to afford the corresponding heterobiaryls **3a**-**3g** in moderate to good yields (53%–82%). This protocol is highly selective, as diverse electron-deficient functionalities such as ketones (**1a**-**1d**), aldehydes (**1e**-**1f**), and nitro group (**1g**) susceptible to undergoing SET reduction could be kept intact during the process. Besides, five-membered ring heteroaryl bromides based on thiophene and furan were well accommodated, leading to the formation of **3h** and **3i** in 77% yield and 71% yield, respectively. Furthermore, this chemistry is effective with pharmaceutically relevant six-membered ring heteroaryl bromides such as 3-bromoquinoline (**1j**) and 6-bromoquinoline (**1k**). The C3 and C6-pyrrole functionalized quinolines **3j**-**3k** can be accessed with high efficiency (68%–75% yields). On the other hand, *N*-methyl pyrroles bearing substituents including aldehyde, ketone, and carboxylic acid at C2 position were tested. While the reaction of 1-methyl-1*H*-pyrrole-2-carboxylic acid did not work, the other two delivered the corresponding 2,5-disubstituted pyrroles in moderate to good yields (**3l**-**3m**, 57%–81%).

Next, the potential of inverse vulcanized polymers to catalyze dual cross-couplings was explored. We chose to investigate the coupling of (hetero)aryl halides with *N*-arylacrylamides, which allows easy access to benzyl-substituted oxindoles frequently encountered in biologically active molecules [51–53]. However, this reaction is challenging due to the multiple competitive processes, such as reduction of aryl bromides, biaryl cross-coupling, and Heck-type cross-coupling. To our delight, with 1-(4-bromophenyl)ethan-1-one (**1a**) and *N*-methyl-*N*-phenylmethacrylamide (**4a**) as the model substrates, the expected transformation involving cascade arylation/cyclization occurred in the presence of IVP-EAE, delivering the corresponding benzyl-substituted oxindole **5a** in 51% yield (Table 2, entry 1). While inferior performance was observed for IVP-DIB and IVP-DCPD, the cascade arylation/cyclization did not take place using either IVP-EG or elemental sulfur as the photocatalyst instead, which is largely attributed to the strong side reactions (Table 2, entries 2–5). Similarly, no reaction occurred in the absence of K_2CO_3 and the lack of H_2O gave a slightly decreased yield (Table 2, entries 6 and 7). Lastly, control experiments verified the indispensability of IVP-EAE, inert atmosphere, and visible light (Table 2, entries 8–10).

Under the standard reaction conditions, IVP-EAE catalyst enabled the cross-coupling of a variety of (hetero)aryl halides and *N*-methyl-*N*-phenylmethacrylamide (**4a**) in good yields (Scheme 4, Top). Aryl halides that contain diverse functionalities including ketones, aldehydes, and nitro groups at various positions were coupled effectively (**5a**-**5f**, 45%–59% yields). Besides, the dual cross-couplings involving six-membered quinolines halogenated at various positions proceeded smoothly, enabling the incorporation of pharmaceutically important quinolines on the 3,3′-disubstituted oxindole scaffolds successfully (**5g**-**5h**, 52%–59% yields).

Then, the scope with respect to *N*-arylacrylamides was examined (Scheme 4, bottom). An array of substrates with varied substitution patterns including both electron-donating and electron-withdrawing groups (MeO-, ^{t}Bu-, Me-, F-, Cl-, Br-, I-, Ac-, CO_2Me-, CN-, CF_3-) at the *para*-position of the aromatic skeletons was tolerated (**6a**-**6k**, 45%–60% yields). For instance, the pharmaceutically important fluorine-containing substituents as well as the halides,

(a) Substrate scope: (hetero)aryl halides

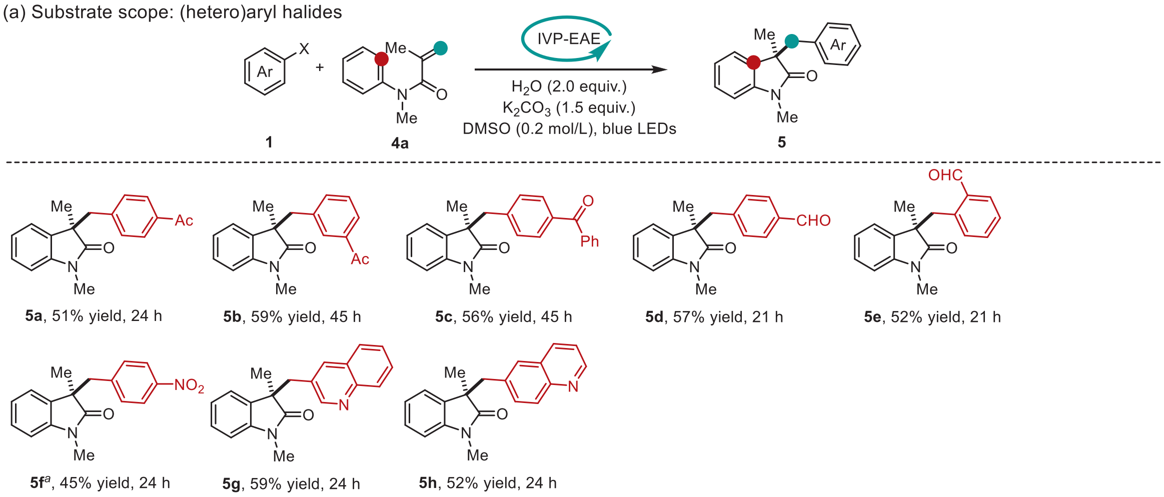

(b) Substrate scope: *N*-arylacrylamides

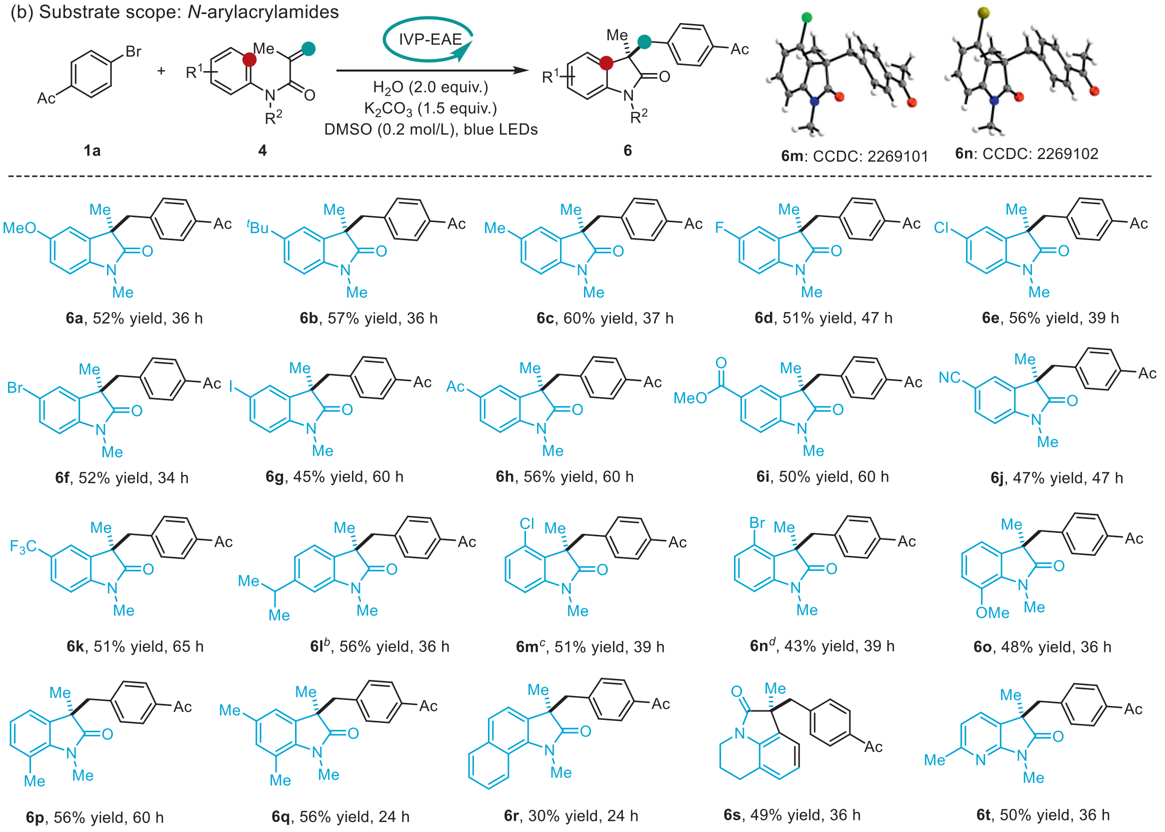

Scheme 4. Substrate scope for dual cross-couplings. Reaction conditions: a solution of IVP-EAE (10.0 mg), **1** (0.2 mmol, 1.0 equiv.), **4** (0.6 mmol, 3.0 equiv.), H_2O (0.4 mmol, 2.0 equiv.), and K_2CO_3 (0.3 mmol, 1.5 equiv.) in DMSO (1.0 mL, 0.2 mol/L) was irradiated by blue LEDs (30 W) at room temperature under nitrogen atmosphere. Unless otherwise noted, (hetero)aryl bromides were used. Isolated yield. ^{a} 1-iodo-4-nitrobenzene was used. ^{b} Ratio of 4- and 6-substituted oxindoles determined by ^{1}H NMR analysis is 1:1.5. The major product **6l** was isolated. ^{c} Ratio of 4- and 6-substituted oxindoles determined by ^{1}H NMR analysis is 1.84:1. The major product **6m** was isolated. ^{d} Ratio of 4- and 6-substituted oxindoles determined by ^{1}H NMR analysis is 1.82:1. The major product **6n** was isolated.

acetyl, and cyano groups which offer additional handles for flexible derivatization could be well retained. Besides *para*-position, the *meta*-substituted (^{i}Pr-, Cl-, Br-) *N*-arylacrylamides were investigated under the optimal conditions. In all the cases, two isomers namely 4- and 6-substituted oxindoles were observed. While the isopropyl-substituted substrate favored the formation of 6-substituted oxindole **6l**, chloro– and bromo–substituted *N*-arylacrylamides afforded 4-substituted oxindoles **6m** and **6n** predominantly. This phenomenon might be attributed to the combined electronic and steric effects of *meta*-substituents. The structures of **6m** and **6n** were unambiguously confirmed by X-ray crystallographic analyses.

Furthermore, the coupling of *ortho*-substituted (MeO-, Me-) *N*-arylacrylamides with 1-(4-bromophenyl)ethan-1-one (**1a**) occurred smoothly, thereby furnishing the corresponding 7-substituted oxindoles (**6o**-**6p**) in 48%–56% yields. Substrates bearing multiple methyl substituents and a naphthalene derivative provided the expected oxindoles **6q**-**6r** with complete selectivity. A tetrahydroquinoline substrate could also be engaged in this transformation, producing the tricyclic benzylated oxindole **6s** in 49% yield. In-

Table 2

Investigation on dual cross-couplings and control experiments.[a]

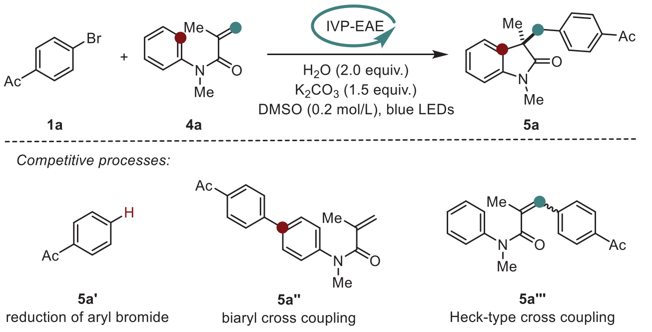

Entry	Variations from standard conditions	Yield (%)[b]
1	None	51 (51)[c]
2	IVP-DIB instead of IVP-EAE	18
3	IVP-DCPD instead of IVP-EAE	28
4	IVP-EG instead of IVP-EAE	0
5	S_8 instead of IVP-EAE	0
6	No K_2CO_3	0
7	No H_2O	41
8	No IVP-EAE	0
9	Air instead of N_2	0
10	No light	0

[a] Reaction conditions: a solution of IVP-EAE (10.0 mg), **1a** (0.2 mmol, 1.0 equiv.), **4a** (0.6 mmol, 3.0 equiv.), H_2O (0.4 mmol, 2.0 equiv.), and K_2CO_3 (0.3 mmol, 1.5 equiv.) in DMSO (1.0 mL, 0.2 mol/L) was irradiated by blue LEDs (30 W) at room temperature under nitrogen atmosphere for 48 h.

[b] Determined by ^1H NMR yield using CH_2Br_2 as an internal standard.

[c] Isolated yield.

triguingly, the pyridine-derived acrylamide underwent the arylation/cyclization cascade with good yield (**6t**, 50% yield), which allowed an unusual C-3 functionalization of pyridine moiety. The quenching experiments with the addition of various scavengers and the proposed pathways for both reactions were depicted in Fig. S5 (Supporting information).

In conclusion, inverse vulcanized polymers (IVPs) have been exploited in catalysis for organic synthesis for the first time. In the presence of a catalytically amount of IVP-EAE derived from cost-effective waste-product elemental sulfur and renewable resource eugenol allylether (EAE), two types of important cross-coupling reactions have been achieved in a transition-metal-free fashion under visible-light irradiation. This protocol allows the rapid assembly of structurally important pyrrole-containing biaryls and 3,3′-disubstituted oxindoles with high selectivity. Further exploration of IVPs in synthetic chemistry are currently underway in our laboratory.

Declaration of competing interest

The authors declare that they have no known competing financial interests or personal relationships that could have appeared to influence the work reported in this paper.

Acknowledgments

We thank the National Natural Science Foundation of China (NSFC, Nos. 22071024, 22271047), the Natural Science Foundation of Fujian Province (Nos. 2021J06020, 2022J011121), the Top-Notch Young Talents Program of China, and the Science and Technology Project of Minjiang University (No. MJY21027) for generous financial support. We thank Dr. Xue Zhou from the Core Research Facilities of CCMS (WHU) for her assistance with Solid-State NMR analysis.

Supplementary materials

Supplementary material associated with this article can be found, in the online version, at doi:10.1016/j.cclet.2023.108832.

References

[1] R. Geyer, J.R. Jambeck, K.L. Law, Sci. Adv. 3 (2017) e1700782.
[2] P. Anastas, N. Eghbali, Chem. Soc. Rev. 39 (2010) 301–312.
[3] Y. Zhu, C. Romain, C.K. Williams, Nature 540 (2016) 354–362.
[4] J.H. Clark, A.S. Matharu, R.E. Hester, R.M. Harrison, Waste as a resource, Issues in Environmental Science and Technology, Royal Society of Chemistry, 2013, pp. 66–82.
[5] T. Mekonnen, P. Mussone, D. Bressler, Crit. Rev. Biotechnol. 36 (2016) 120–131.
[6] G. Kutney, Sulfur: History, Technology, Applications & Industry, 2nd Ed, ChemTec Publishing, 2013.
[7] J. Lim, J. Pyun, K. Char, Angew. Chem. Int. Ed. 54 (2015) 3249–3258.
[8] J.J. Griebel, R.S. Glass, K. Char, et al., Prog. Polym. Sci. 58 (2016) 90–125.
[9] M.J.H. Worthington, R.L. Kucera, J.M. Chalker, Green Chem. 19 (2017) 2748–2761.
[10] J.M. Chalker, M.J.H. Worthington, N.A. Lundquist, et al., Top. Curr. Chem. 377 (2019) 16.
[11] Y. Zhang, R.S. Glass, K. Char, et al., Polym. Chem. 10 (2019) 4078–4105.
[12] J.M. Chalker, M. Mann, M.J.H. Worthington, et al., Org. Mater. 3 (2021) 362–373.
[13] T. Lee, P.T. Dirlam, J.T. Njardarson, et al., J. Am. Chem. Soc. 144 (2022) 5–22.
[14] W.J. Chung, J.J. Griebel, E.T. Kim, et al., Nat. Chem. 5 (2013) 518–524.
[15] A.G. Simmonds, J.J. Griebel, J. Park, et al., ACS Macro Lett. 3 (2014) 229–232.
[16] I. Gomez, O. Leonet, J.A. Blazquez, et al., ChemSusChem 9 (2016) 3419–3425.
[17] J.J. Griebel, N.A. Nguyen, S. Namnabat, et al., ACS Macro Lett. 4 (2015) 862–866.
[18] J.J. Griebel, S. Namnabat, E.T. Kim, et al., Adv. Mater. 26 (2014) 3014–3018.
[19] M.P. Crockett, A.M. Evans, M.J.H. Worthington, et al., Angew. Chem. Int. Ed. 55 (2016) 1714–1718.
[20] R.A. Dop, D.R. Neill, T. Hasell, Biomacromolecules 22 (2021) 5223–5233.
[21] J. Xuan, W.J. Xiao, Angew. Chem. Int. Ed. 51 (2012) 6828–6838.
[22] C.K. Prier, D.A. Rankic, D.W.C. MacMillan, Chem. Rev. 113 (2013) 5322–5363.
[23] D. Ravelli, S. Protti, M. Fagnoni, Chem. Rev. 116 (2016) 9850–9913.
[24] Y. Li, M. Wang, X. Jiang, ACS Catal. 7 (2017) 7587–7592.
[25] Y. Chen, L.Q. Lu, D.G. Yu, et al., Sci. China Chem. 62 (2019) 24–57.
[26] Y.P. Wu, M. Yan, Z.Z. Gao, et al., Chin. Chem. Lett. 30 (2019) 1383–1386.
[27] C. Dai, B. Liu, Energy Environ. Sci. 13 (2020) 24–52.
[28] Y. Luo, Z.Y. Xu, H. Wang, et al., ACS Macro Lett. 9 (2020) 90–95.
[29] Z.Y. Xu, Y. Luo, H. Wang, et al., Chin. J. Org. Chem. 40 (2020) 3777–3793.
[30] S. He, X. Chen, F. Zeng, et al., Chin. Chem. Lett. 31 (2020) 1863–1867.
[31] F. Wang, S.Y. Wang, Org. Chem. Front. 8 (2021) 1976–1982.
[32] M. Yang, H. Han, H. Jiang, et al., Chin. Chem. Lett. 32 (2021) 3535–3538.
[33] H. Li, X. Li, J. Zhou, et al., Chin. Chem. Lett. 33 (2022) 3733–3738.
[34] P. Xiang, K. Sun, S. Wang, et al., Chin. Chem. Lett. 33 (2022) 5074–5079.
[35] S.H. Yang, J.C. Song, H. Yang, et al., Chin. Chem. Lett. 34 (2023) 108131.
[36] Z. Lei, F. Xue, B. Wang, et al., Chin. Chem. Lett. 35 (2024) 108633.
[37] B. Zhang, S. Petcher, R.A. Dop, et al., J. Mater. Chem. A 10 (2022) 13704–13710.
[38] A. Hoefling, D.T. Nguyen, Y.J. Lee, et al., Mater. Chem. Front. 1 (2017) 1818–1822.
[39] R. Morales-Cerrada, S. Molina-Gutierrez, P. Lacroix-Desmazes, et al., Biomacromolecules 22 (2021) 3625–3648.
[40] S.D. Roughley, A.M. Jordan, J. Med. Chem. 54 (2011) 3451–3479.
[41] D.G. Brown, J. Boström, J. Med. Chem. 59 (2016) 4443–4458.
[42] J.S.M. Lee, A.I. Cooper, Chem. Rev. 120 (2020) 2171–2214.
[43] C.C.C.J. Seechurn, M.O. Kitching, T.J. Colacot, et al., Angew. Chem. Int. Ed. 51 (2012) 5062–5085.
[44] I. Ghosh, L. Marzo, A. Das, et al., Acc. Chem. Res. 49 (2016) 1566–1577.
[45] I. Ghosh, T. Ghosh, J.I. Bardagi, et al., Science 346 (2014) 725–728.
[46] I. Ghosh, B. König, Angew. Chem. Int. Ed. 55 (2016) 7676–7679.
[47] L. Marzo, I. Ghosh, F. Esteban, et al., ACS Catal. 6 (2016) 6780–6784.
[48] T. Constantin, F. Juliá, N.S. Sheikh, et al., Chem. Sci. 11 (2020) 12822–12828.
[49] H. Li, X. Tang, J.H. Pang, et al., J. Am. Chem. Soc. 143 (2021) 481–487.
[50] N. Shen, R. Li, C. Liu, et al., ACS Catal. 12 (2022) 2788–2795.
[51] K. Ding, Y. Lu, Z. Nikolovska-Coleska, et al., J. Med. Chem. 49 (2006) 3432–3435.
[52] M.S. Christodoulou, F. Nicoletti, K. Mangano, et al., Bioorg. Med. Chem. Lett. 30 (2020) 126845.
[53] J. Majhi, A. Granados, B. Matsuo, et al., Chem. Sci. 14 (2023) 897–902.